Characterization and mobility of arsenic and heavy metalsinsoils polluted by the destruction of arsenic-containingshells from the Great War

Hugues Thouin, Lydie Le Forestier, Pascale Gautret, Daniel Hube, Valérie Laperche, Sébastien Dupraz, Fabienne Battaglia-Brunet

Characterization and mobility of arsenic and heavy metalsinsoils polluted by the destruction of arsenic-containingshells from the Great War

Hugues Thouin[a,b], Lydie Le Forestier [b], Pascale Gautret [b], Daniel Hube [a], Valérie Laperche[a], Sebastien Dupraz [a],Fabienne Battaglia-Brunet [a,b].

[a]BRGM, 3 avenue Claude Guillemin, 45060 Orléans, France

[b]Universitéd'Orléans, ISTO, UMR 7327, 45071 Orléans, France, and CNRS, ISTO, UMR 7327, 45071 Orléans, France, and BRGM, ISTO, UMR 7327, BP 36009, 45060 Orléans, France

Highlights

- Examination of the complex legacy of chemical shell destruction
- Amorphous phase identified as main As, Cu and Zn carrier
- Unexpected mineralogical associationobserved
- Potential for bacterial As(III) oxidation detected
- As stability driven mainly by adsorption to hydrous ferric oxides (HFO)

Graphical abstract

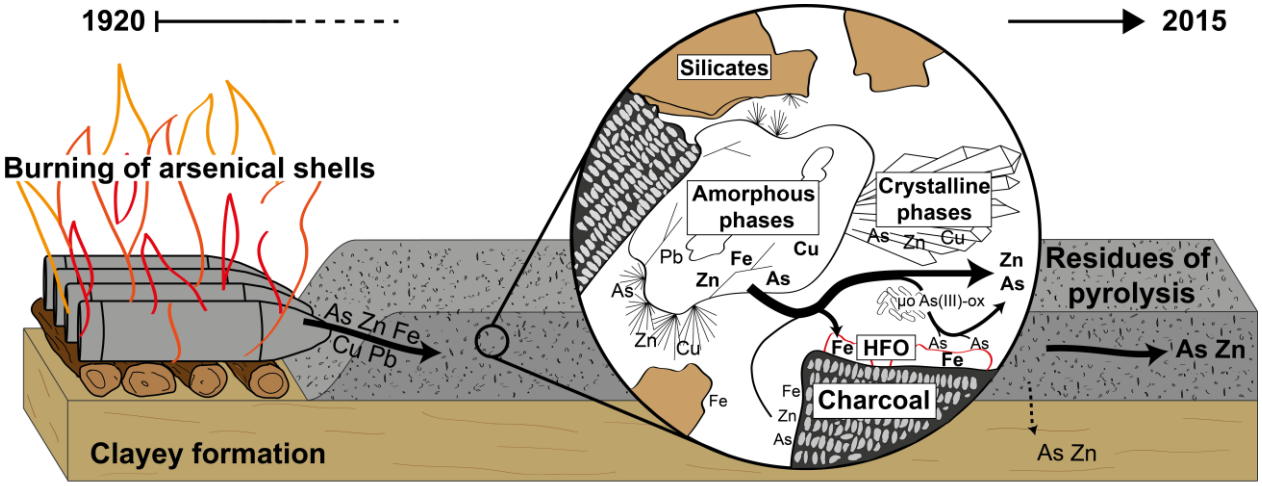

Abstract

Destruction of chemical munitions from World War I has caused extensive local top soil contamination by arsenic and heavy metals. The biogeochemical behavior of toxic elements is poorly documented in this type of environment. Four soils were sampled presenting different levels of contamination. The range of As concentrations in the samples was 1,937–72,820 mg/kg. Concentrations of Zn,Cu and Pb reached 90,190 mg/kg, 9,113 mg/kg and 5,777 mg/kg, respectively. The high clay content of the subsoil and large amounts of charcoal from the use of firewood during the burning process constitutean ample reservoir of metals and As- binding materials.However, SEM-EDS observations showed different forms of

association for metals and As. In metal-rich grains, several phases were identified: crystalline phases, where arsenate secondary minerals were detected, and an amorphous phase rich in Fe, Zn, Cu, and As. The secondary arsenate minerals, identified by XRD, wereadamite and olivenite (zinc and copper arsenates, respectively) and two pharmacosiderites. The amorphous material was the principal carrier of As and metals in the central part of the site. This singular mineral assemblage probably resulted from the heat treatment of arsenic-containing shells.Microbial characterization included total cell counts, respiration, and determination of As(III)-oxidizing activities. Results showed the presence of microorganisms actively contributing to metabolism of carbon and arsenic, even in the most polluted soil, therebyinfluencing the fate of bioavailableAs on the site. However, the mobility of As correlated mainly with the availability of iron sinks.

Keywords: Chemicalammunition destruction, Soil contamination, Metals, Arsenates, Microbial As(III)-oxidation

1. Introduction

Almost 100 years after the end of the First World War the scars of battle can still be observed along the front line. Hupy andSchaetzl (2008) have studied the effect of shelling on soil structure and landscape recovery after the conflict. The First World War was the first incidence of major warfarethat made massive use of chemical weapons. However, very little informationis availableon the chemical impacts of the conflict on soil, groundwater or wildlife. High concentrations of metals in living organisms and the presence of perchlorate in groundwater along the red zone nevertheless reflect a real impact of this war on the environment (Hube, 2013; Prefectoral decree, Pas de Calais, 25 October2012).

In the early 2000s, several sites where First World War chemical weapons were destroyed were found to be contaminated by inorganic pollutants.Only two of these wereinvestigated: the first is located in Belgium (BausingerandPreuss, 2005), the secondis northeast of Verdun, in France (Bausinger*et al*., 2007).Chemical shells were disposed of by burning on both of these sites during the 1920s. The munitions destroyed were mainly "blue cross shells" containing organoarsenic warfare agents.The Belgian burning ground has since been used for agriculture (Bausinger and Preuss, 2005) but the French site, named "Place-à-Gaz", has been unaffected by human activities and undisturbed since destruction of the shells.

Bausinger*et al*. (2007) showed that the "Place-à-Gaz" had locally limited but severe soil contamination by arsenic, zinc, copper and lead, with concentrations reaching respectively 150 g/kg, 130 g/kg, 15 g/kg and 25 g/kg.The metals came from various parts of the munitions. Shells contained mainly iron, while fuses, driving bands and shell casings were made from copper or zinc.Lead was used for shrapnel balls, primary explosives and chemical warfare equipment. "Blue cross shells" were filled with diphenylchloroarsine (Clark I) and diphenylcyanoarsine(Clark II).These organoarsenic molecules were probably oxidized during

the combustion, releasing huge amounts of inorganic arsenic into the surrounding environment.Bausinger*et al*. (2007) estimated that, over a century, most of the arsenic oxides have been transformed into arsenates or sorbed onto iron oxides or clays, abundant in the inherited soil.

The primary factor influencing mobility of heavy metals in these soils appeared to be pH (Bausinger*et al*., 2007).Under the site conditions,the soil pH varied from 5 to 6, whichfavored Cu and Pbfixation in soil, while Zn was more mobile and leached. Arsenic was less affected by pH and behaved differentlyfrom metals. However, As concentrations in interstitialwaters (c_{mean}=838 µg/L) were significantly higher than themaximum contaminant level (MCL) of arsenic in drinking water as recommended by the World Health Organization (WHO) in 1993, i.e. 10 µg/L. The mobility of Ason the site thus required further investigation.

Arsenic is mainly found in the environment asinorganic species, arsenate As(V) and arsenite As(III) (Cullen and Reimer, 1989).Microbial activities play a major role in As speciation in soil. Different bacterial mechanisms are responsible for As(III) oxidation or As(V) reduction (Santini*et al*.,2000, Stolz*et al*., 2002), thus altering Asmobility, toxicity and bioavailability (Pierce and Moore, 1982, Masscheleyn*et al*., 1991). The bacterial activity on former ammunition destruction sites has not been documented to date,but biogeochemistry may explain As speciation and mobility in such environments.

Organic matter, which can have high concentrationsin soil (up to 25%), may drive the mobility of metals and arsenic on the site (Bausinger*et al*., 2007).Indeed, the organic compounds may containadsorption or complexation sites or induce methylation of metals and metalloids (Saada*et al*., 2003, Park*et al*., 2011, Huang *et al*., 2012). The presence of organic matter also affects bacterial activity. A recent study has shown that As(III)-oxidizing activity

in polluted soil can be influenced by the amount of bioavailable organic matter (Lescure *et al*., In press).

Bausinger*et al*. (2007) explored the mobility of inorganic pollutants in the "Place-à-Gaz" ground materialby sequential extractions. These experiments provided indirect information on the carrier phases but no direct information was available on the mineralogy of soil materials. Moreover, arsenic speciation was not directly determined and no data were available on the activity of microorganisms in this type of heavily polluted soil. Our work focused on the mineralogy, particle size and the geochemistry ofthe "Place-à-Gaz" surface soils,in order to better understand the behavior of inorganic pollutants on sites polluted by the destruction of chemical weapons. These data were alsolinked with the mobility of pollutants and biogeochemical parameters.

2. Materials and methods

2.1. Study site

The study site, known as "Place-à-Gaz", is located in the Spincourt forest, 20 km northeast of Verdun, France (Bausinger*et al*., 2007). At the end of the First World War large amounts of shells and ammunition were stored in the region. In 1920, the Pickett andFilscompany was commissioned by the French Ministry of War to destroy these munitions. 200,000 German chemical shells were opened and burned inpiles at the center of this area in 1928. The fire was fueled by wood covered with explosive materials.

2.2. Chemical characterization and soil sampling

Total concentrations of As, Cu, Zn and Pb were determined in situ using XL3t800 NITON© portable X-ray fluorescence field apparatus (pXRF), in order to defined the metal(loid)s distribution and to targeted the soil sampling. The signals were calibrated with the chemical

analyzes of the soil samples and considered the soil moisture. Maps of As, Cu, Zn and Pb concentrations were drawn by interpolating data by kriging (ArcGIS©).

Four soilswere sampled inthe surface, non-saturatedblack layer (0–10 cm) in zones with contrasting vegetation cover. The soils were sieved at 2 mm through sterile sieves, placed in in sterile glass jarsand stored at 5°C. Their water content was determined by drying at 105°C for 24h. In order to study the chemical composition of different particle size fractions, soil sub-samples wereseparated into three fractions by mechanical sieve shaker: coarse sand (>200 µm), fine sand (50–200 µm) and loam and clay (<50 µm).

2.3. Soil chemistry and mineralogy

For chemical and mineralogical analyses, the raw soils and particle fractions were ground to 70 µm. Major elements were determined by inductively coupled plasma (ICP) atomic emission spectroscopy (AES) using a Thermo Fischer ICap 6500; trace elements were determined by ICP-mass spectrometry (MS) on a SiexPerkin-Elmer Elan 5000a, both analyses being conducted at the *Service d'Analyses des Roches et des Minéraux* (*SARM* – rock and minerals analysis unit of the *CRPG-CNRS*national research institutes). Prior to analysis, the samples were fused with $LiBO_2$and dissolved in a mixture of 1 N HNO_3, H_2O_2 and glycerol. Organic carbon (C_{org})and total S were also determined at the SARM center, by carbon and sulfur determination on a Leco SC144 DRPC(SARM, CRPG-CNRS). The mineralogical composition was determined by X-ray diffraction (XRD). XRD patterns were recorded between 0° and 90° (2θ) at a scan rate of 0.3° 2θ cm^{-1} using an INEL CPS120 diffractometer equipped with a Co anode (Co $K\alpha_1$ = 1.78897 Å).

Scanning electron microscopy (SEM) and energy dispersive X-ray spectroscopy (EDS) were performed to explore the composition and distribution of metals and As in the four soils. SEM was performed on a TM 3000 accompanied by a SwiftED3000 X-Stream module (Hitachi),

and operated at 15 kV accelerating voltage. The acquisition time of EDS analyses was 300 s per sample.

2.4. Leaching and percolation tests

Leaching tests provide information about the mobility of metal and Asfrom soil towards the water phase. The fourwet soil sampleswere mixed with ultrapure water, with a solid/liquid ratio of 1 to 10 (wet soil equivalent to 25 g dry soil, 250 mL of ultrapure water), and the tubes were rotated on a roller mixer for 24 h. The leaching solutionswere filtered at0.45 µm then acidified with 10% of HNO_3. Fe, Cu, Zn and Pbconcentrationswere determined using an atomic absorption spectrophotometer (AAS, Varian, Palo Alto, CA, USA).

The leaching test was not suitable for evaluation of the speciation of soluble As, because some As(III)maybe oxidized during the 24 hleaching test. A percolation test was performed to determine the speciation of soluble As in conditions close to those of the site. The soil (as wet soil equivalent to 1 g dry soil)was placed in a 5 mL syringe (diameter 13 mm) equipped with a rock wool stopper, without packing. Percolation experiments were performed in triplicate for each soil. 25 mL of a weakly mineralized spring water (Mont Roucous, pH 5.85; 3.1 $mg.L^{-1}$ Na^+; 2.4 Ca^{2+}; 0.5 Mg^{2+}; 2.0 SO_4^{2-}; 6.3 HCO_3^-; 3 NO_3^-), used to simulate rain water, was fed in drops onto the surface of the soil in the syringe. Percolation water was recovered and filtered at 0.2 µm. As(III) and As(V) were immediately separated using an ion exchange method (Kim, 2001). Separation was performed on anionic resin (AG 1-X8©, Biorad, Hercules, CA, USA). A sample of percolation water filtered at 0.2 µm was acidified for total As determination. Arsenic was quantified with an AAS oven (Varian, Palo Alto, CA, USA).

A specific leaching test was applied to particles coated with materials in the amorphous phase. Soil particles, previously observed by SEM, were incubated in

0.25 Mhydroxylammoniumchloride and 0.25 MHClfor10 minutes. The particles were observed again by SEM after the leaching step.

2.5. Bacterial enumeration

Total bacteria were extracted from soils using a Nycodenz gradient separation method(Bertrand *et al*., 2005) and enumerated after fluorescent DAPI staining, as described in Kumar *et al*. (2013).

As(III)-oxidizing bacteria were enumerated by the Most Probable Number method.The soil (as wet soil, equivalent to 0.2 g dry soil) was placed in a sterile, glass Erlenmeyer flask with 10 mL of sterile physiological saline (9 $g.L^{-1}$NaCl in demineralized water), agitated for 30 min at 25°C, then sonicated 2 x 20 s at 45 kHz. Triplicate suspensions were prepared for each soil. The soil suspension was diluted in stages in sterile physiologicalsaline to a dilution of 10^{-7}. CAsO1 mineral medium (Battaglia-Brunet *et al*., 2002) containing 100 $mg.l^{-1}$As(III) was distributed over Microtest TM Tissue culture plates (96 wells), 250 µLper well. Each well was inoculated with 25 µL of diluted soil suspension. Five wells were inoculated with each dilution. Culture plates were incubated at 25°C for 10 days. The presence of As(III) in the wells was revealed by the formation of As(III)-PyrrolidineDithioCarbamate (PDC), an insoluble white complex: 150 µL of 0.1 M acetate buffer (pH 5) and 100 µL PDC solution (5 $g\ L^{-1}$)were added to each cell. A white precipitate appeared when As(III) was present, i.e. when As(III)-oxidizing bacteria were absent (negative well). Non-inoculated wells served as negative blanks while wells containing CAsO1 medium with 100 $mg.L^{-1}$As(V)provided a positive reference.The number of positive wells for each dilution was determined, and the most probable number of bacteria in dilutions was givenby Mc Grady table for five tubes.

2.6. As(III)-oxidizing activity tests

The four samples were incubated at 25°C for 72 h before starting the tests. The As(III) oxidizing tests were performed in 250 mL Erlenmeyer flasks filled with 100 mL of CAsO1 medium (Battaglia-Brunet *et al*., 2002) supplemented with 1 mMAs(III) and inoculated with a mass of material equivalent to 0.2 g of dry weight. Flasks were plugged with cotton to retain oxidizing conditions and were incubated at 25° under agitation (100 rpm). The flasks were sampled each day, and twice a day during As(III) oxidation. Samples were filtered at 45 µm and frozen at -20°C until As(III)/As(V) separation was performed. Tests were performed in triplicate.As(V) was quantified by flame AAS(Varian, Palo Alto, CA, USA), after As(III)/As(V) separation with the PDC/MIBK method (Battaglia-Brunet *et al*., 2002). First order As(III) oxidizing rate constants were determined by linear regression fitting of the As(V) versus time line, during the reaction.

2.7. Mineralization of biological carbon

The biodegradability of intrinsic organic matter was studied via CO_2 emission (soil respiration),as per Rey *et al*.(2005). The equivalent of 100 g of dry weight, adjusted to 80% of water holding capacity, was placed in 250 mL serum flasks. Samples were incubated at 25°C. After one week of stabilization, flasks weresealed hermetically with rubber stoppers andgas samples were taken weekly for 5 weeks via the septum with a double-needle blood collection tube and a vacuum tube (Vacuette®, Greiner Bio-one). The soil moisture was kept constant by adjusting the water content to the initial mass each week.CO_2 concentration in the gas phase was analyzed with a Varian 3400 gas chromatograph using thermal conductivity detection.

Carbon mineralization rates were calculated from the linear increase of CO_2 concentration in flasks over time. The specific carbon mineralization rate was calculated as the carbon mineralization rate / total soil organic carbon ratio.

2.8. Statistical tests

Statistical analyses were performed using the XLSTAT (Addinsoft) software. Data were tested for homogeneity of variance and normal distribution. One-way analysis of variance (ANOVA) and Tukey HSD (Honestly Significantly Different) tests werecarried out to test for any significant differences between the means.Differences between means at the 5% level ($P<0.05$) were considered significant.

3. Results

3.1. Site characterization

The "Place-à-Gaz" has a surface area of 2000 m² (Fig.1.a.1). The soil surface is covered by a black layer containing slag, coal, ash and residues from the pyrolysis of munitions (Fig.1.a.2). The thickness of this layer varies from a few centimeters at the edge of the zone to around 40 cm at the center of the site (Fig.1.a.3). The substrate beneath theblack layer is a clayeyWoëvre formation (Callovian age) with a thickness of around 200 m. These clays seriously limit the infiltration of rainwater, which will tend to run off to wetlands in low-lying areas at the periphery of the site (Fig.1.a). The height of annual precipitation in the study area is 758 mm and the annual average temperature is 10.7 °C (data from Météo France, Metz station).

The central part of the site has not been colonized by plants (Fig.1.a and 1.c). The first colonizing species was*Pohlianutans*mosses. A species of lichen, *Cladoniafimbriata,* and an herbaceous plant,*Holcuslanatus,* are implanted on the outer areas, growing on mosses. The surface area of the bare zone seems to have declined since the Bausinger*et al*. (2007)study, indicating progressive revegetation of the site.

The central part of the burned area was heavily contaminated by zinc, copper and arsenic. Intensity of contamination decreased progressively towards the edge of the forest, as shown

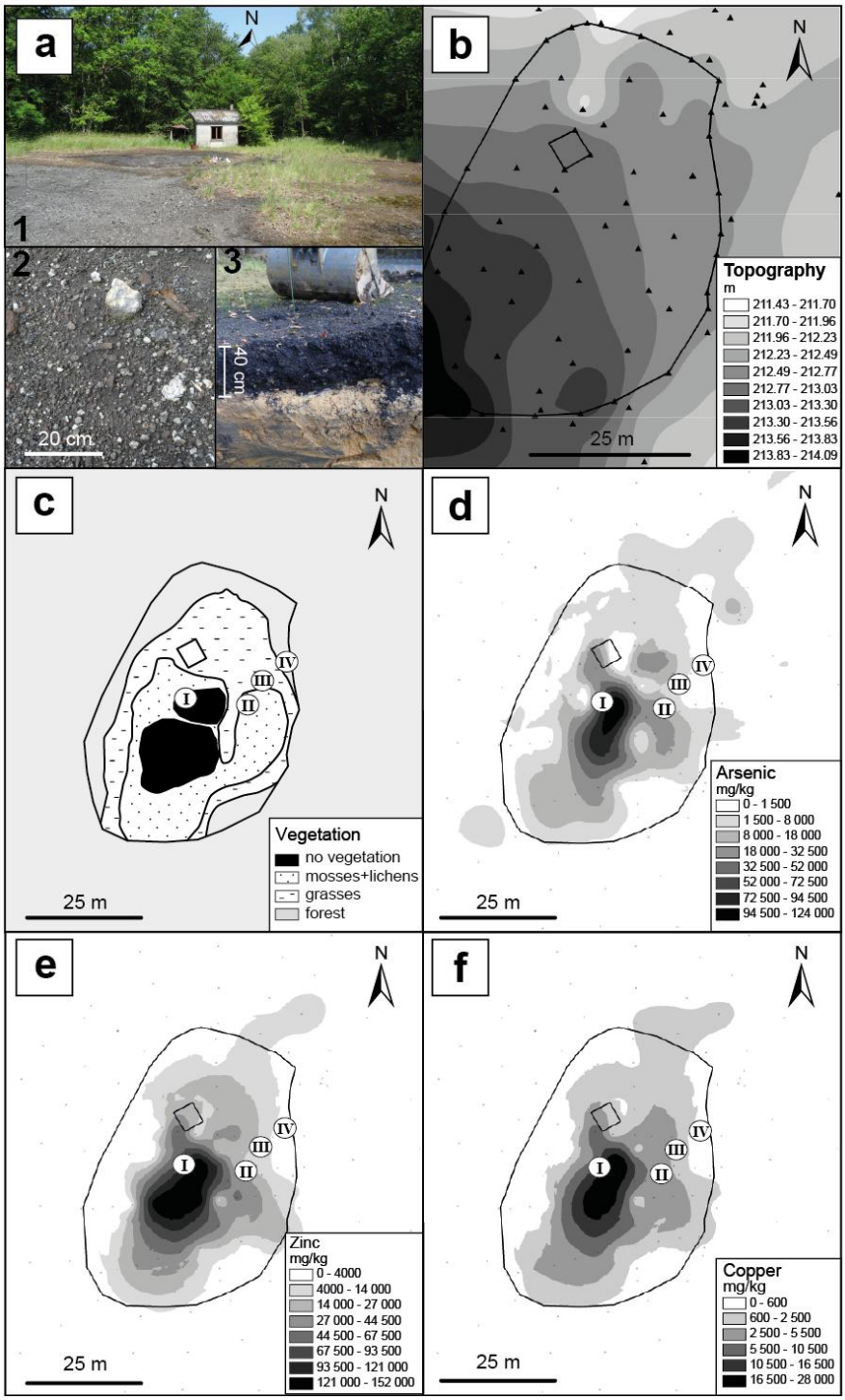

Fig.1: Situation and contamination of the study site
(a.1): overview of the "Place-à-Gaz"; (a.2): black layer surface; and (a.3): soil profile with black layer overlying Woëvre formation clays. **(**b): topography of the study area. (c): implantation of vegetation. Roman numerals represent soil sample locations. (d,e,f): maps of concentrations of As, Zn and Cu at the soil surface, measured with pXRF.

by As, Cu and Zn maps (Fig.1.d, e and f). For Pb mapping(given in SM.1) the interpolating kriging was conducted with five high-Pb-concentration measuring pointsin the northeast of the site, at the extremity of the sampling fields, which induced a nugget effect. These high Pb concentrations were measured in a peripheral deposit of shell fragments; however, the pollution gradient was still observable in the burned ground.

3.2. General soil characteristics and elemental composition

The four soil samples studied were taken from zones with contrasting pollution levels and different vegetation cover (Fig.1.c, d, e and f): soil I, with no vegetation, was the most contaminated; soil II, covered by mosses and lichens, was less contaminated; soil III was covered by grasses; and soil IV, covered by forest vegetation and humus, was the least contaminated.

Tab. 1: Chemical analyses of the four soil samples. CS: coarse sand. FS: fine sand. L&C: loam and clay.

		Major (%)										**Trace (mg/kg)**							
Sample	Particle size fractions	SiO_2	Al_2O_3	Fe_2O_3	CaO	K_2O	P_2O_5	MnO	MgO	Corg	S total	As	Cu	Pb	Zn	Ba	Cd	Cr	Sn
I	Bulk	13.62	2.29	11.13	0.61	0.42	0.38	0.10	0.15	25.87	0.13	72820	9113	3830	90190	743.4	158.9	57.6	308.1
	CS	6.65	1.86	14.87	0.51	0.23	0.35	0.09	0.11	21.58	0.14	74870	12680	4331	152200	448.4	224	40.6	324.3
	FS	16.16	2.64	11.97	0.6	0.5	0.44	0.10	0.18	21.12	0.12	83090	8929	4526	84520	779.1	127.3	56.3	318
	L&C	26.06	3.09	10.17	0.59	0.71	0.39	0.09	0.20	19.89	0.1	67270	7331	3661	68330	993.4	109.1	104.6	323.6
II	Bulk	50.15	4.83	6.19	0.64	1.22	0.29	0.06	0.28	12.26	0.11	30840	5082	5777	37310	453.4	76.8	77.1	138.8
	CS	18.24	3.39	12.26	1.1	0.56	0.4	0.09	0.29	23.33	0.21	57840	8736	9325	61730	477.8	136	58.5	219.7
	FS	42.57	4.54	6.92	0.72	1.11	0.34	0.08	0.29	14.39	0.14	41900	6501	8012	40210	502.9	95.9	69.5	175.5
	L&C	66.17	5.48	4.08	0.49	1.52	0.21	0.04	0.29	5.63	0.07	21310	3106	3927	23610	465.1	48.1	98.7	109.1
III	Bulk	69.61	6.72	4.99	0.45	1.75	0.18	0.07	0.42	3.69	0.04	6253	1591	2528	10660	296.1	18	84.4	45.9
	CS	61.11	6.7	10.66	0.79	1.64	0.21	0.12	0.46	4.03	0.06	9793	3009	4379	19550	395.2	30.5	94.5	71.9
	FS	69.19	6.52	4.53	0.44	1.76	0.2	0.07	0.41	4.26	0.05	8480	1863	3620	12610	380.2	23.9	97.1	56.6
	L&C	75.85	6.8	2.9	0.38	1.83	0.15	0.04	0.40	2.55	0.03	4055	1078	2102	7257	345.3	12.9	120.1	34.9
IV	Bulk	58.85	7.2	4.08	0.62	1.73	0.27	0.15	0.53	8.44	0.07	1937	1451	968	13270	312.5	26.2	97.3	43.6
	CS	36.41	5.77	7.63	0.88	1.2	0.4	0.32	0.47	17.3	0.1	3612	2795	2007	24540	262.9	49.7	79.8	59.7
	FS	52.89	7.13	4.34	0.64	1.65	0.33	0.22	0.55	10.64	0.08	8469	2042	1427	12670	354.3	30.1	89.7	48.4
	L&C	67.57	7.5	3.42	0.47	1.88	0.21	0.07	0.52	5.3	0.05	1436	991.8	646	9284	321.8	17.6	111.8	39.2

All four soils contained 25–40% of fine sand (SM.2) but soil IV had a different texture with a lower proportion of coarse sand and a higher proportion of fine particles (clay and loam). The lowest proportion of fine particles was found in soil I.Electrical conductivity was similar for all soils (around 10 $mS.cm^{-1}$)but the pH of soil I (5.3) was lower than that of the others (5.8–5.9).

Concentrations of elements in the surface material samples are given in Table 1.Contamination of the soilsby As, Zn and Cu decreased in the following order: sample I< sample II < sample III < sample IV.Concentrations of As vary between 72,820 and 1,937 mg/kg, Zn concentrations between 90,190and 10,660 mg/kg and Cu concentrations between 9,113 and 1,451 mg/kg. Lead behaved differently, with a greater concentration in sample II: 5,777 mg/kg.Metals and arsenic were found mainly in the coarse and fine sand fractions, while Si, Al and K were most present in the loam and clay fraction. An important concentration of organic carbon was measured in sample I: 25.87%.

3.3. Textural characterization, microscopic observation and EDS analysis

Several types of grains were observed in the four soils. Millimetric to micrometric grains with tabular structure were observed in all soils, as well asaggregates of the smallest grains (Fig.2.a).These grains,presentin greater proportions in soils III and IV, were identified as potassic and sodic aluminosilicate phases. No traces of metal(loid)s, except Fe, were detected by EDS analyses.Black grains, mainly in soils I and II, presented a wood structure with cell porosity, and high carbon contents (Fig.3b). These grains were indentified as charcoals. Many micrometric particles were present at the charcoal surfaces, and may be composed by a mixture of Si, Al and Cl, associated with small amounts of metal(loid)s (Fe, Zn, As).

Whiteand/orgreen-blue crystalline materials were observed in the macroporosity of soil I, and were characterized by a prismatic texture (Fig.3.a and b), on an acicular texture(Fig.3.c and d). As revealed by SEM/EDS analyses, the prismatic crystals mainly contained O, Zn and As (Fig.4.a), whereas acicular minerals were composed of an assemblage of O with Zn, As and Cu (Fig.4.b).The soil I was also characterized by large amorphous phases (Fig.3.e, f, g and h), with contrasting colors (yellow, red, white), covering diverse soil particles (charcoal, silicates, metallic fragments of shells), and forming aggregates. The surface of the amorphous phasespresented semi-spherical nodules and micro-cracks (Fig.3.f). The agglomerates of micrometric spheres were also observed in the porosity (Fig.4.c), and are

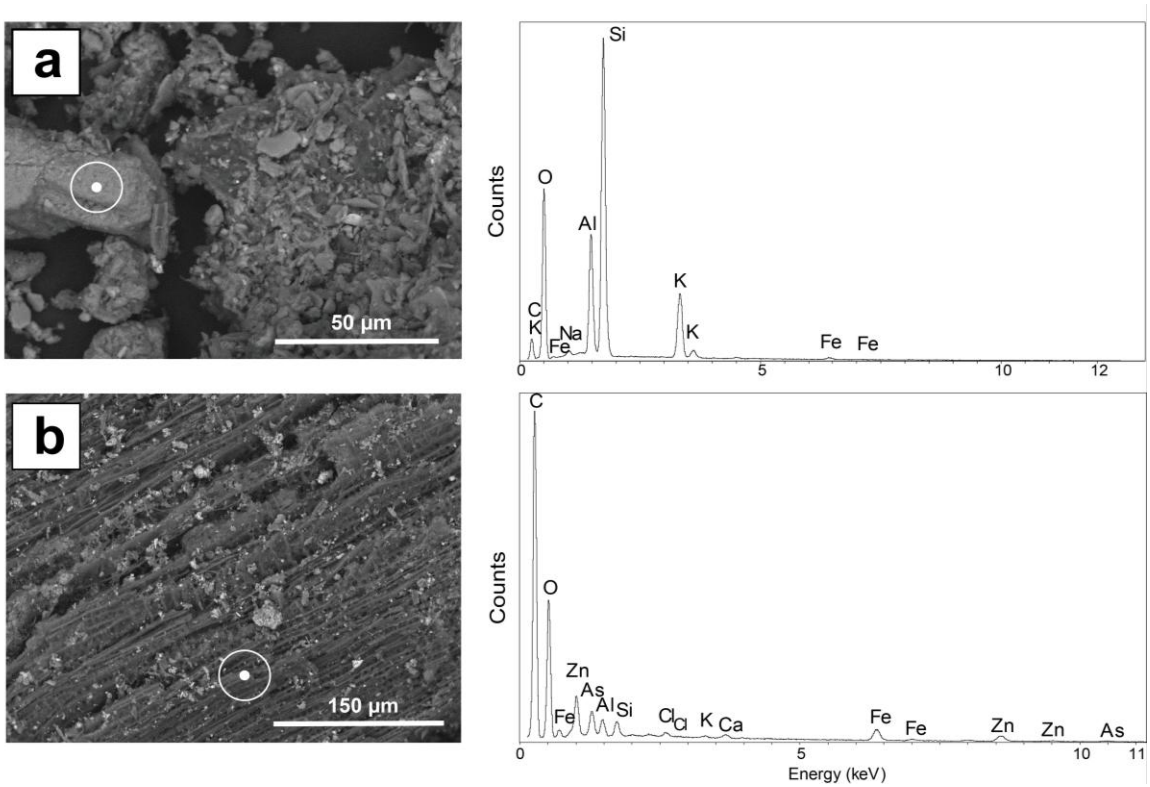

Fig. 2: Observation and composition of inherited silicates and charcoals from black layer

(a): backscattered electron images and EDS spectrum of a silicate mineral from soil sample IV. This grain was mainly composed of Si, Al and O. K and Na were also detected. The only metal(loid) detected was Fe. (b): SEM picture and EDS analysis of a charcoal grain from soil sample I. These grains were identifiable by their woody structure, and contain carbon associated with. The EDS spectrum indicated charcoal containing many small quantities of elements, particularly Fe, Zn and As. The targets correspond to the location of EDS elemental analysis.

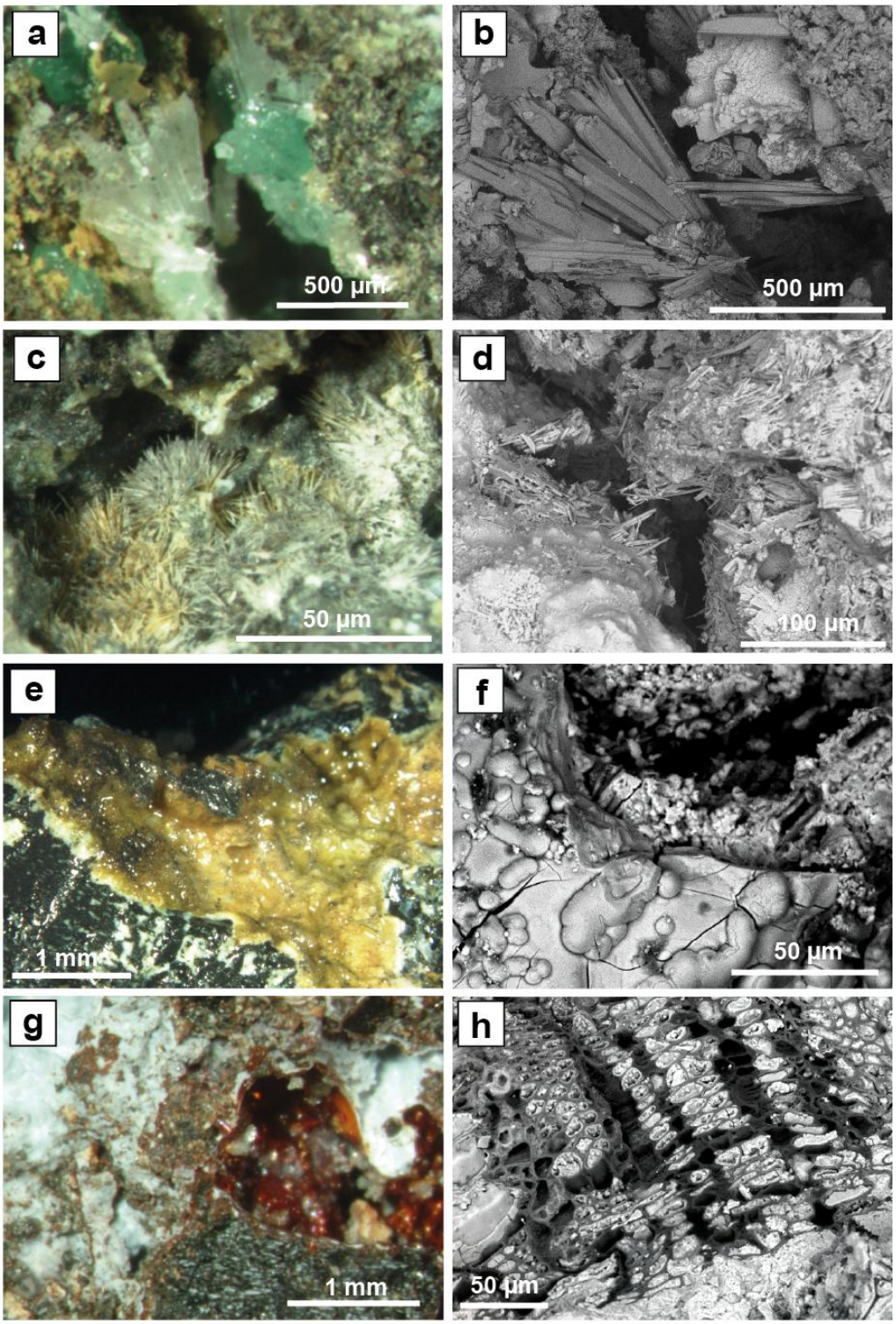

Fig. 3: Microscopic pictures of crystalline and amorphous phases of soil sample I.

On the left, (a,c,e and g) binocular magnifier pictures, and on the right (b,d,f and h) SEM pictures. (a) and (b): white prismatic crystals and green-blue crystals formed in the porosity. (c) and (d): white acicular crystals with radial intergrowth. (e): grain of charcoal covered with yellow amorphous phase. Its surface was smooth. (f): SEM view of surface of the amorphous phases. This one is covered by semi-spherical nodules and micro-cracks. (g): white and red amorphous phases close to a charcoal grain whose porosity was filled by white amorphous phases. (h): high-resolution image of this wood charcoal.

composed by a blend of Fe, As, Zn, Cu and Al(Fig.4.c).Incubation ofgrains, from soil sample I, in hydroxylammonium chloride and HCl resulted in the total or partial dissolution of the amorphous material(Fig.5).

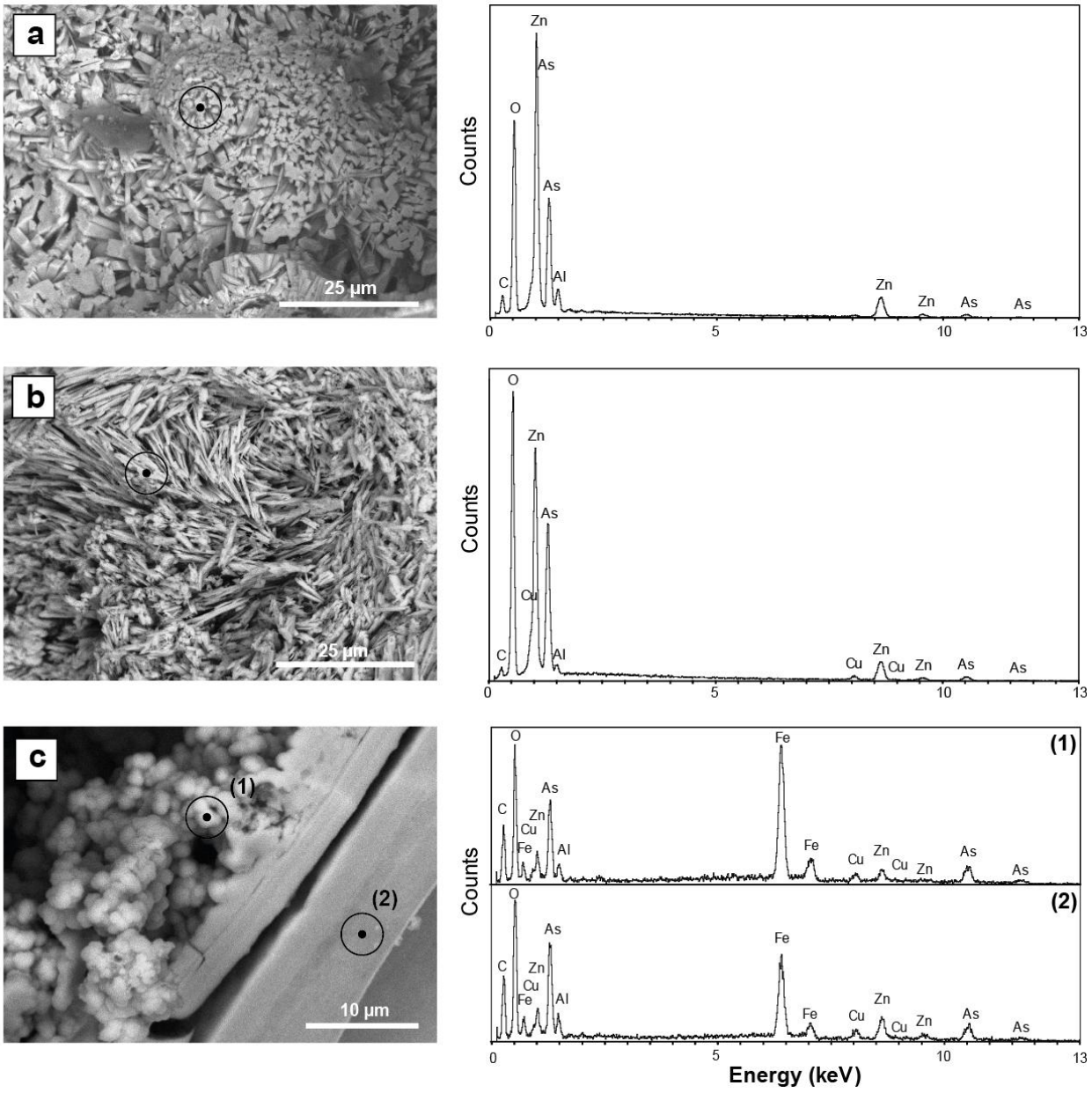

Fig. 4: Observation and composition of crystallized mineral and amorphous phase carriers of metal(loid)s

Soil sample I SEM images with elemental spectra of As carrier crystallized minerals with Zn (a) and Zn + Cu (b). (c): iron-rich amorphous phases with spheres, carrier of As, Cu and Zn. The targets correspond to the location of EDS elemental analysis.

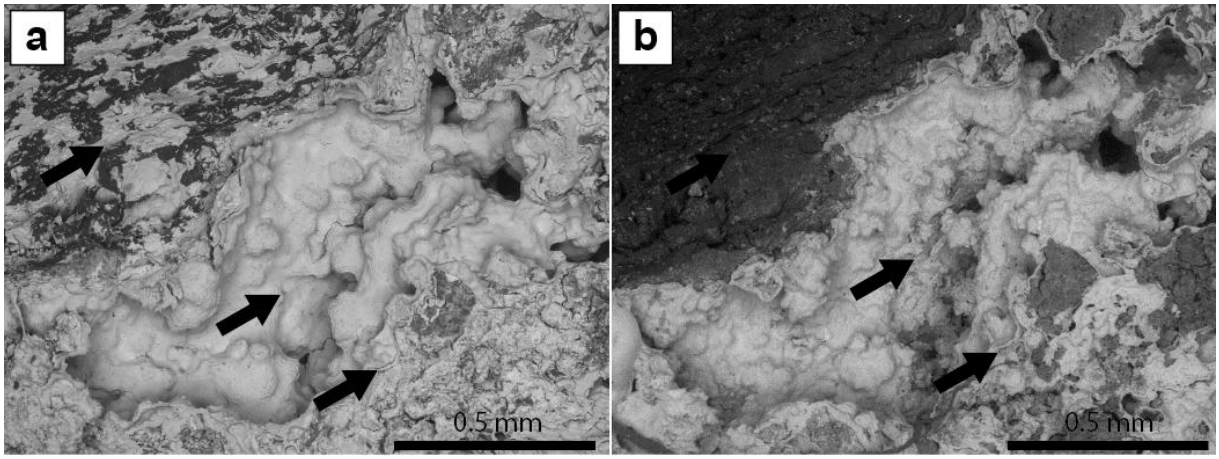

Fig. 5: SEM pictures showing effect of hydroxylammonium chloride andHCl on amorphous phases of soil sample I.

(a): grain of soil covered by amorphous phase. (b): the same sample after 10 minutes in 0.25 M hydroxylammonuim chloride + 0.25 HClsolution. The amorphous phases that covered charcoal (top arrow) and silicate grains (bottom arrow) were totally dissolved. The surface of the thicker amorphous phase covering the cavity (middle arrow) was partially dissolved.

3.4. Soil mineralogy

The crystallized phases from the four samples were investigated by XRD analysis for the different size fractions (Fig.6). Quartz, a ubiquitous mineral,was present in the four soils.Potassium and sodium feldspars were detected in samples from soilsII, III and IV. Clays weredetected in soil IV, particularly in its fine fraction, however the mineralogy of the clay could not be defined. In soil I, four secondary arsenic mineralswere identified: adamite ($Zn_2AsO_4(OH)$),olivenite ($Cu_2AsO_4(OH)$), Na-pharmacosiderite ($NaFe_4(AsO_4)_3$ $(OH)_5$5H2O) and Ba-pharmacosiderite ($BaFe_4(AsO_4)_3(OH)_5$5H_2O). The zinc and copper arsenates were more abundant in the coarse sands fraction. The pharmacosiderite mineralswere mainly present in the silts and clays fraction. A zinc oxide, zincite (ZnO), was also identified in the bulk and coarse sand fraction. Soil I also gave a significant XRD background signal, suggestingan important amorphous phase.

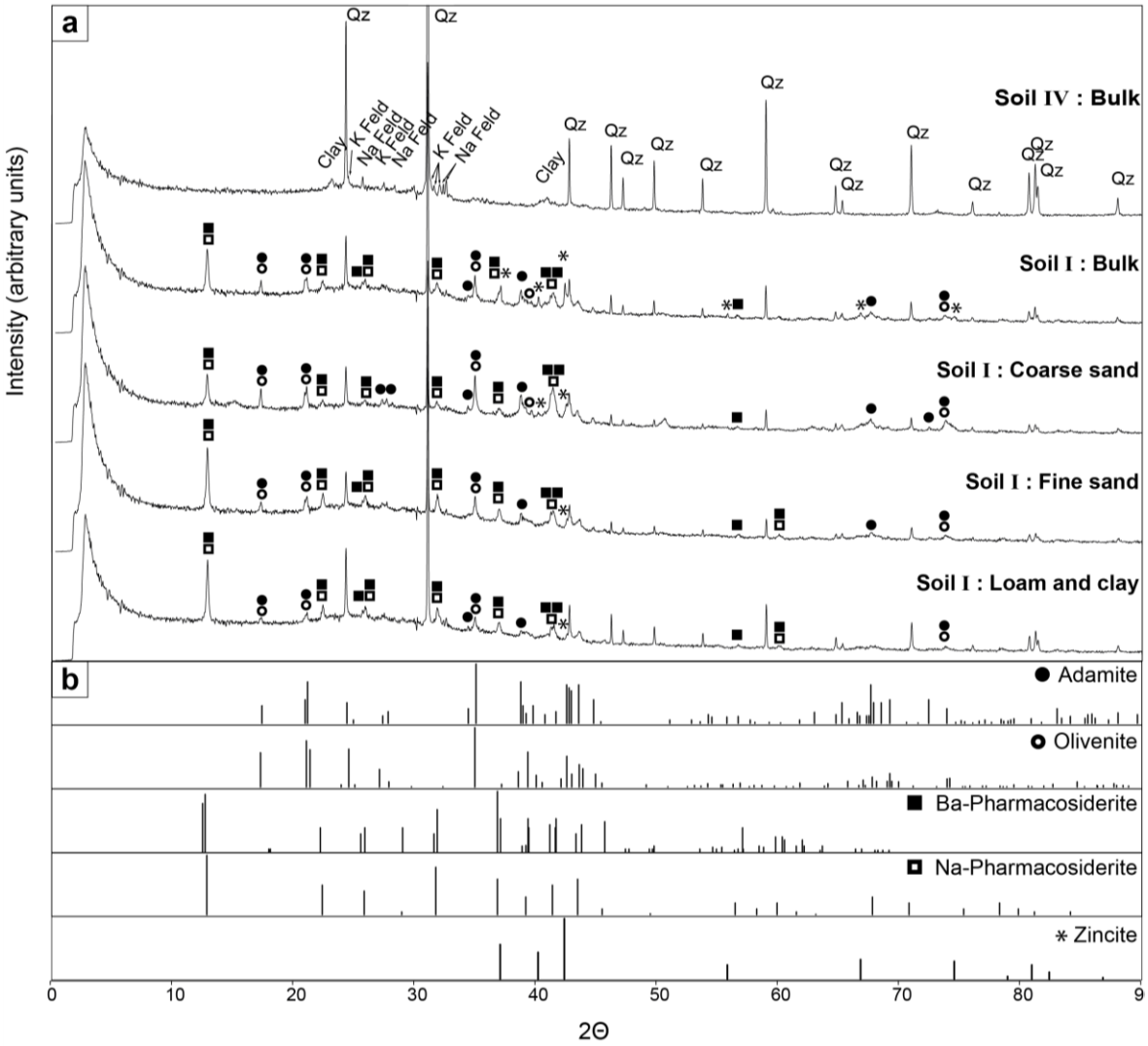

Fig. 6: Mineralogy of soils sample I and IV

(a): X-ray diffractograms of bulk sample of soil IV and of each particle size fraction of soil sample I: Qz = quartz (ICDD 46-1045); Na Feld = sodium feldspar (ICDD 19-1184); K Feld = potassium feldspar (ICDD 31-0966). (b): standard XRD patterns of the five reference mineral carriers of metals and As detected in soil I: Adamite (ICDD 39-1354); Olivenite (ICDD 42-1353); Ba-Pharmacosiderite (ICDD 34-0154); Na-Pharmacosiderite (ICDD 38-0388); Zincite (ICDD 36-1451).

3.5. Mobility of contaminants

The mobility of As, Zn, Cu, Pb and Fe was assessed by leaching with water in batch systems (Tab.2). Concerning the absolute quantities of leached elements, Assolubility was significantly higher in soil I than in the other soils and As was less leachable in soils III and IV. The concentrations of soluble Cu and Pb were similar in all soilsand the mobility of Zn was higher in soil I than in the other soils. Focusing on the proportion (%) of each leached

element compared to its total concentration in the solids, the mobility in closed (batch) systems was overall low (<1.5%), however it was higher in all cases for soils III and IV than for soils I and II.

Tab. 2: Leaching test. Solubility of metal(loid) contaminants of samples after 24h batch leaching tests with ultrapure wat. Amounts of leached elements were expressed as milligrams per kilogram of dry soil. The proportion of leached pollutants was expressed as percentage of total pollutant concentrations in the soils.

	As			Fe			Cu			Pb			Zn		
Sample	mg/kg		%	mg/kg		%	mg/kg		%	mg/kg		%	mg/kg		%
I	77.2	a	0.11	39.1	a	0.04	3.0	a	0.03	2.9	a	0.08	103.9	a	0.12
II	40.5	b	0.13	27.2	b	0.04	2.8	a	0.05	4.6	a	0.08	70.8	ab	0.19
III	21.8	c	0.35	35.1	ab	0.07	2.8	a	0.17	4.2	a	0.17	59.9	b	0.56
IV	26.3	c	1.36	30.6	ab	0.07	3.0	a	0.21	2.2	a	0.22	74.5	ab	0.56

Values are the means (n=3). Values with different letters are significantly different (P<0.05, ANOVA, Tukey-HSD)

A different tendency was revealed by the percolation experiment (Tab.3): with this open and short-term system, mobile As concentration decreased from 2,202 µ/L in soil I to 28 µg/L in soil IV; the proportion of mobile As was highest in soil II and lowest in soilIV.

Tab. 3: Parameters related to As speciation. Arsenic speciation in the solid phases of the four bulk soils (solid), speciation in water from percolation tests (liquid), and enumeration of specific As(III)-oxidizing micro-organisms (µo) (bacteria).

			I		II		III		IV	
Solid	**$As(III)_{total}$**	mg/kg	1577	a	852	b	191	c	29	c
	$As(V)_{total}$	mg/kg	70178	a	36846	b	7355	c	1954	c
	Ratio of $As(III)_{total}$	%	2.25	a	2.33	a	2.41	a	1.48	a
	As_{total}/Fe_{total}	mol As/mol Fe	0.48		0.37		0.09		0.04	
Liquid*	**As_p**	µg/L	2202	a	1627	b	141	c	28	c
	$As(III)_p$	µg/L	97	a	39	b	<10		<10	
	$As(V)_p$	µg/L	2106	a	1588	b	134	c	25	c
	Ratio of As total $_p$	%	0.075		0.13		0.056		0.036	
	Ratio of $As(III)_p$	%	4.5	a	2.5	b	-		-	
	pH		5.34		5.95		5.84		5.92	
Bacteria**	**As(III)-ox µo**	Bact/g dry soil $\times 10^3$	1.93	a	1.47	a	10.35	a	5.92	a
	Ratio of As(III)-ox µo***	‰	0.165	a	0.049	ab	0.043	ab	0.012	b

Values are the means (n=3). Values with different letters are significantly different (P<0.05, ANOVA, Tukey-HSD). (*) percolation tests. (**) in the bulk soils, (***) ratio specific As(III)-oxidizing µo/total µo.

As(V) was the main As speciesin all soils (Tab.3). Despite significant differences in absolute As(III) and As(V) concentrations in the four soils, the proportion of As(III) was constant at around 2%. Another species of arsenic was detected in all soils butdidnot correspond to monomethylarsonate, dimethylarsinate or arsenobetaine.As(V) was also the dominant form (Tab.3) in aqueous phases of percolation tests. The proportion of mobile As(III) was low (less than 5%), but significantly higher in soil I compared to soil II.

3.6. Biogeochemical parameters

Although microbial As(III) oxidation began earlier in the less polluted soils III and IV (Fig.7a), the As(III)-oxidation rate was significantly higher in the most polluted soils I and II (Fig.7b).The total bacterial concentration was significantly higher in soils III and IV than in soils I and II. Whereas the absolute concentration in As(III)-oxidizing bacteria was in the same range for the four soils, the percentage of active As(III)-oxidizing bacteria, in the whole bacterial community, was higher in the most polluted soil I (Tab.3).

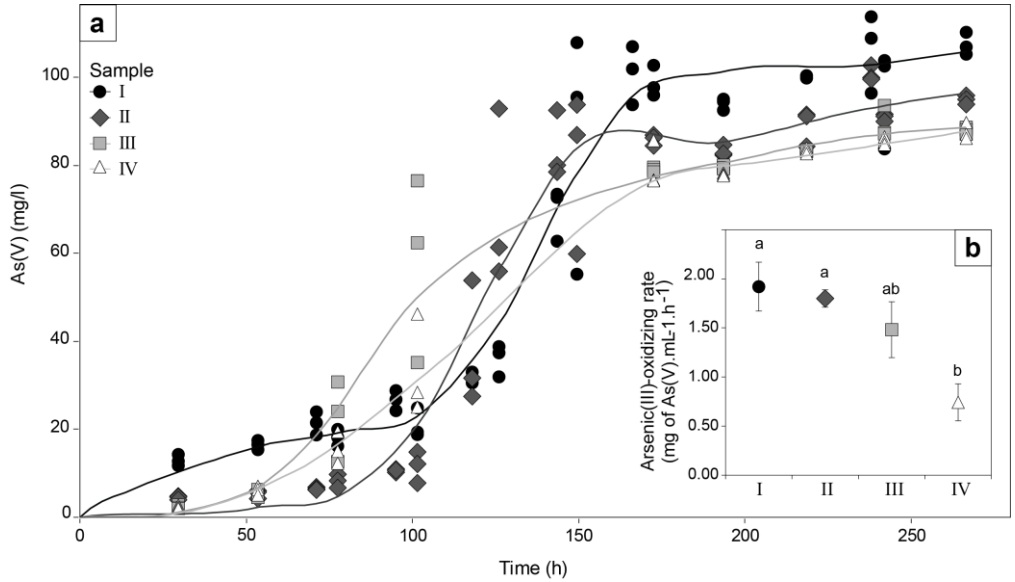

Fig. 7: **Bacterial As-III oxidizing activities**
(a): evolution of As(V) concentration during the As(III)–oxidizing activity tests performed with triplicates on the four soils. (b): As(III) oxidation rates corresponding to the previous activity tests. Error bars represent the standard deviation of the mean of three replicates. Different letters denote significant difference between samples ($P < 0.05$, ANOVA, Tukey-HSD).

Carbon mineralization was significantly more rapid in soil IV(25.17 ± 2.07 µg C-CO_2 g^{-1}dry mass day^{-1}) and in soil I (19.01 ± 0.52 µg CO_2 g^{-1}dry mass day^{-1}) than in the two other samples (Fig.8a). Rates measured for II and III soils were about five times lower.However, as the intrinsic carbon content varied greatly from one soil to another, the data were also expressed as specific mineralization rates (Fig.8b). The specific carbon mineralization rate was therefore not significantly different in soils I and II (73 ± 2 µg CO_2 g^{-1}Corg $day^{-1}$and 58 ± 1 µg CO_2 g^{-1}Corg day^{-1},respectively). Specific carbon mineralization of soil IV remained the highest.

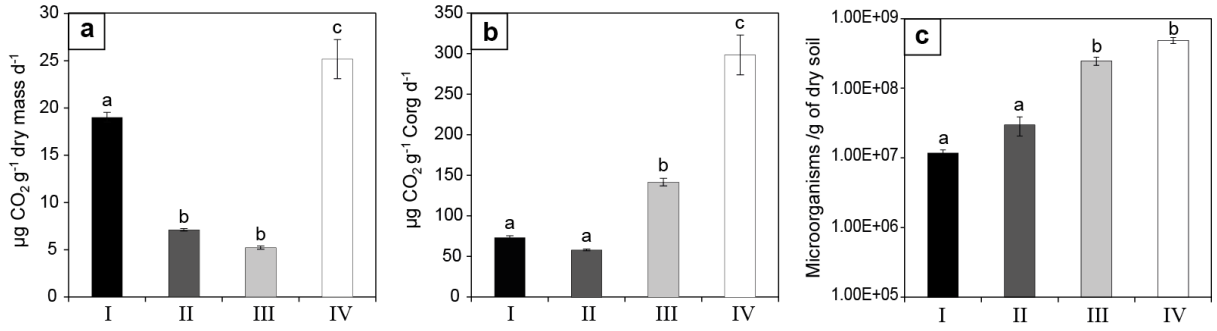

Fig. 8: Biological carbon mineralization

(a): carbon mineralization rates of the four contaminated soils. (b): specific carbon mineralization rates (carbon mineralization rate / organic carbon concentration ratio). (c): total microorganisms concentration. Error bars represent the standard deviation of the mean of three replicates; Letters denote significant difference between samples ($P < 0.05$, ANOVA, Tukey-HSD).

4. Discussion

4.1. Environmental contamination caused specifically by the thermal treatment of gas shells

The “Place-à-Gaz” wa mainly contaminated by arsenic, copper, zinc and lead. The different parts of the containers of chemical shells probably constitute the sources of the heavy metals Cu, Zn and Pb. As contamination, on the other hand, was derived from the oxidation

ofdiphenylarsines contained in “blue cross shells” during the combustion process. Besides the considerable amount of contaminants, the samples of the surface black layer contained high concentrations of organic carbon (Tab.1).Bausinger*et al*. (2007) have suggested that organic carbon had two origins; the humic matter provided by the forest and the charcoalresulting from the use of firewood during the thermal treatment.Here, the carbon mineralization rates confirm the presence of two types of organic matter (Fig.8): bioavailable organic matter in the less polluted soil, which can be attributed to humic matter; and less bioavailable organic matter in the central part, corresponding to charcoal.

The subsoil of the Woëvre-plain (Fig.1.a.3) is formed from clay and other silicates. The concentrationsof Si, Al and K, mainly present in the fine fraction of the four soils (Tab.1), and the detection of Na and K feldspars and clays in soil V (Fig.6) confirmed the presence of inherited silicates in the black layer.During and after the incineration treatment, metals and metalloids werereleased into an environment rich in iron, clay and charcoal, three substances known for their capacity to bind inorganic contaminants (Bradl, 2004). The spatial and mineralogical relationships between these substances and contaminants were investigated in the four soils.

Traces of As, Zn and Fe were detected in the charcoal fragments (Fig.2.b). However, the results of SEM-EDS analyses performed on different grains of the four soils attested that As and heavy metals were not principally bound to charcoals or silicates.The observations of crystalline and amorphous materials containing large quantities of metals and arsenic suggestedcommon carriers for inorganic contaminants. The white and blue crystallized materials with prismatic structures with radial intergrowths (Fig.3,a-d and Fig.4.a,b) certainly correspond to minerals of the Adamite-Olivenite series ($(Zn\text{-}Cu)_2AsO_4$ (OH)) detected by XRD (Fig.6). Two other arsenates were identified in the most contaminated soil: Na-pharmacosiderite ($NaFe_4(AsO_4)_3(OH)_{5,}$ 5H2O) and the Ba-

pharmacosiderite($BaFe_4(AsO_4)_3(OH)_5\,5H_2O$). These arsenic carrier minerals are usually found as secondary minerals resulting from the alteration of primary minerals such as arsenopyrite and have been observed most frequentlyin post-mining environments (Morin *et al*., 2002, Drahota and Filippi, 2009, Haffert*et al*., 2010).To our knowledge, the present study is the first to revealsuch a mineral association in a context of incineration of hazardous materials. However, the sequential extraction performed by Bausinger*et al*. (2007) showed that most of the As, Zn, Cu and Pbwere not hosted by crystallized fractionsyet,in the central part of the site, the majority of As, Cu, Pb and Zn were leached by hydroxylammonium chloride and HCl. This leached fraction was attributed to species bound to amorphous Fe-oxyhydroxides (Hall *et al*., 1996). DRX and SEM-EDS resultshighlighted the presence of amorphous material composed mainly of Fe but also containingimportant amounts of As, Cu and Zn. Moreover, this amorphous phase was leached by hydroxylammonium chloride and HCl (Fig.5) and can thus be attributed to the amorphous Fe-oxyhydroxides fraction mentioned by Bausinger*et al*. (2007) as a major carrier of pollutants, detected indirectly by a selective extraction procedure. Consequently, the amorphous phase observed directly here was probably the principal carrier of arsenic and metals in the central parts of the "Place-à-Gaz".

Several indices suggested that the nature of the carrier phases was directly related to the incineration of chemical shells. The structure of the amorphous phase was the first sign that a significant high temperature was reached during destruction. The micro-cracks, observed on the surface(Fig.2.f), were certainly formed as the material cooled. Moreover, the small spherical particles in soil pores (Fig.4.c) present similar morphology as particles observed in fly ashes produced by incenerators(Fisher *et al*., 1978, Le Forestier*et al*., 1998).In addition,pharmacosideritehas a zeolite structure (Baur*et al*., 2012) and many authors have detected zeolite forms in incineration ashes (Shigemoto*et al*., 1993, Murayama *et al*., 2002, Querol and al., 2002). Zincite(ZnO) indentified in thesoil I is a synthetic mineral found

typically in metallurgical furnace residues. Sidenko*et al*. (2001) have observed the presence of zincite in the self-combustingwaste heaps of a zinc smelting plant.The presence of amorphous materials, small spherical particles, zeolite-like structures of pharmacosiderite and zincitethereforesuggestedthat the mineralogical associations in the polluted soil were driven by the incinerationof shells. First, the combustion oxidized organoarsenicmolecules and smelted metals from shell containers, resulting in the formation of an iron and oxygen-rich amorphous phase covering grains of the inherited soil. Theseamorphous material wasthe main carrier of As, Cu, and Zn. Then, during cooling, the secondary arsenate minerals (Adamite, Olivenite and pharmacosiderite) and zincitecrystallized in the material pores.Furthermore, the presence of iron in the amorphous phase can be used to estimate that the maximum combustion temperature was above the melting point of iron, i.e. 1,538°C. Such an amorphous mineral phase, mainly composed of iron, oxygen, arsenic and heavy metals, hadnever been observed before this study.

4.2. Mobilityof contaminants

Contamination of the site by As, Cu, Pb and Zn was significant but very localized. As, Cu and Zn (and to a lesser extent Pb) were distributed along a concentration gradient from the center of the site, devoid of vegetation, towards the forest (Fig.1.c-f). In June 2014, during the sampling campaign,wetland zones were observed in the periphery of the “Place-à-Gaz”, resulting from meteoritic water accumulation at low topographic points,because of the very low permeability of the Woëvre formation clays. This formation, beneath the heavily contaminated black layer, limited the vertical transfer of metals and As, forming a natural barrier to infiltration of rainwater. The higher pH (above pH 7), in the clay horizon also formed a chemical barrier to the mobility of metals, especially Zn (Bausinger*et al*., 2007). Transfer of contaminants on the site was therefore mainly driven by runoff water at the base of the highly permeable black layer. The contaminated area at the northern low topographic

point of the site, outside the burningzone, showed this horizontal transfer (Fig.1.b and Fig.1.d-f).

The solubility of the main carrier phases of metals and arsenic was difficult to predict since, while the solubility constants of adamite and olivenite are documented (K_{sp}equal to 5.71 for adamiteand 2.39for olivenite, Magalhães*et al*., 1988), no solubility or thermodynamic data are available for pharmacosiderite minerals (Drahota and Filippi, 2009). Moreover, the stability of the amorphous phase was unknown. The potential mobility of metals and arsenic was first evaluated by leaching tests (Tab.2). Leached Cu and Pbvalues seemed to reach a threshold independently of the original ground level pollution (Tab.2).The percentage of leached pollutants were very low (below 2%), however theyrevealed that a higher proportion of pollutants were mobilizedfrom the less contaminated soil. These observations can be explained by the saturation of these elements in the aqueous phase of the leaching batch systems, which would induce their re-precipitation. In order to evaluate the mobility of metals and arsenic in these conditions, the geochemical PHREEQCi3.0.6.7757 code together with the minteq.v4thermodynamic database was used by integrating the complete chemistry of the leached water (SM3). In these acid (5<pH<6) and oxidizing conditions,the PHREEQCi simulation, integrating the chemical parameters and concentrations of major and trace chemical species of the leached water, highlighted that hydroxides and oxides containing Cu,Pb and Feshould precipitate (SM.3). This could explain the low mobility of Cu and Pb in the environmental conditions of the site.Conversely, according to the PHREEQCisimulation, no mineral containing arsenic or zinc should precipitate but iron minerals known to efficiently adsorb As (ferrihydrite, goethite) should precipitate. Where the behavior of zinc, is concerned, these results are consistent withthe Bausinger*et al*. (2007)study concludingthat the moderately acidic soil pH allowed mobilization ofconsiderable amounts of Zn.However, Bausinger*et al*.

2007 did not explain the behavior of arsenic, as no simple correlationbetweenAs mobility and pH could be found.

Arsenic concentrations in water obtained with the percolation test (Tab 3) were in the same range than those measured by Bausinger*et al.* (2007) in soil interstitial water samples (mean value of 838 µg/L and maximum value of 2377 µg/L).The proportion of As(III) in the percolation water of the most polluted soil was greater than the proportion of As(III) in the corresponding solid. This can be explained by the high mobility of arsenitewhich has no charge at this pH range, unlike the arsenate (Smedley and Kinniburgh, 2002). However, in soil II the proportion of As(III) in the percolating water was not higher than in the solid phase. This result can be explained by the difference of pH between soils I (5.3) and soil II (5.9), as differential As(III) and As(V) adsorption behavior is very sensitive to pH in this range. At pH 5–6, As(V) sorbs more readily to amorphous hydrous ferric oxides (HFO) than does As(III) (Dixit and Hering, 2003) and thus tends to immobilize As. However, adsorption of As(III) increases with pH, while adsorption of As(V) shows an opposing trend This may explain why more As(III) was released by soil I than by soil II.

Biological As(III) oxidation may decrease the proportion of As(III). As(III)-oxidizing tests (Fig.7) and enumeration of specific As(III)-oxidizing organisms (Tab.2) revealed the potential for bacterial As(III) oxidation in all soils. However, the longer time lapse in As(III)-oxidizing activity tests in soil I than in other soils shows that this activity may be inhibited because of the high concentrations of toxic elements. This toxicity clearly influenced the total bacterial concentration and microbial activities (i.e. organic matter mineralization; Fig.8) that were significantly lower in soils I and II than in soils III and IV. The High Cu concentration in soil I may explain the lower microbial numbers and the lower microbial activities involved in C-mineralization process (Flemming and Trevors, 1989). Thus, the relative inhibition of

microbial As(III) oxidizing activity may have contributed to the higher proportion of As(III) released from soil I compared to soil II.

However, the elevated toxic element concentrations seemed to have exerted a selective pressure on the microbial communities, as suggested by the high As(III)-oxidizing rates observed with microbial populations from soils I and II (Fig.7) and by the highest proportion of As(III)-oxidizing microorganisms compared to the total bacterial concentration in soil I (Tab.2).

Concerning total As mobility, the batch leaching test (Tab. 2) resulted in a higher mobility from soils III and IV, contrary to the percolation experiment (Tab. 3), which indicated a maximum As mobility in soil II. This apparent contradiction can be explained by the difference in experimental procedure. In the batch leaching test, the contact time between water and soils allowed the leaching and re-precipitation of iron that induced As removal through adsorption on fresh HFO, the absolute iron concentration being higher in soils I and II than in soils III and IV (Tab.1). This phenomenon explains why in batch leaching tests the percentage of final soluble As was higher with soils III and IV. Conversely, the percolation test was rapid (less than 1 hour), and the percolating water was immediately filtered and acidified; re-precipitation of solubilized iron was, therefore, probably limited. In the percolation conditions, the mobility of As was most probably governed by the molar ratio As/Fe and pH of the soils.

Dixit and Hering, (2003) gave values of site density for As adsorption on HFO :between 0.2 and 0.3 mol sites per mol Fe. The molar ratio As/Fe in the center of the “Place-à-Gaz” was greater than 0.3 (Tab.3), suggesting that the adsorption sites for As in the soils I and II were saturated. Thus, As should be more mobile in soils I and II than in soils III and IV. Lastly, the higher mobility of As from soil II than from soil I in percolation tests may be explained by

soil pH: soil I was more acidic than soil II, yet As(V) adsorption onto iron oxides continuously decreases when pH increases between 3.5 and 10 (Dixit and Hering, 2003).Thus, As(V) was less strongly adsorbed onto Fe-rich particles in soil II than in soil I.

Then, the adsorption of Asonto the HFO in the most contaminated part of the site was not enough to immobilize the whole amount of arsenic. At the periphery of the site, where the As/Fe ratio was less than 0.2, a significant decrease of mobile arsenic was detected in the percolating water. Batch leaching and percolation experiments yielded different and complementary information concerning As mobility in the soils: percolation testing represents the short-term mobility occurring when rainwater passes rapidly through the permeable surface soil, whereas the leaching test mimics the phenomena that probably occur in the stagnant water retained in the saturated areas.On the whole, these results suggest that bacterial As(III) oxidation contributes to reduce the proportion of As(III) in soil pore water but that the adsorption of As onto HFO was the major phenomenon driving the short-term mobility of As.

5. Conclusion

The present study has provided newinformation about the carriers of arsenic and heavy metals in soils strongly polluted by the historical incineration of chemical weapons.

Nearly one century after the polluting event, arsenic speciation shown by SEM-EDS and XRD was proven to be directly linked to the incineration of shells. Indeed, the two main As-carriers were identified as amorphousmaterials composed of a blend of metals and secondary arsenate minerals that were formed in the pores of the material as it cooled.Such amorphous carriers of arsenic and heavy metals, with high iron content and no silica but presenting a glass-like morphology, were observed here for the first time.

The soils of the “Place-à-Gaz” site were strongly contaminated by As, Zn, Cu and Pb, the more mobile of these pollutants being Zn and As. The mobility of Zn was probably governed primarily by pH, whereas As behavior seems to be related to pH, As/Fe ratio, Fe dissolution / precipitation processes and microbial activities.

The long-term exposure to high levels of toxicity in soils I and II, and particularly in soil I, exerted a selective pressure on the microbial communities that probably tended to select organisms with high As(III)-oxidizing efficiency and increased the proportion of As(III)-oxidizing bacteria in the global community.Thus, microbes can contribute to maintaining of a high proportion of AsV on site. However, the microbial activity studied, i.e. organic matter mineralization and As(III) oxidation, are less active in the most polluted soils compared to those with lower concentrations in inorganic pollutants, suggesting that the inorganic pollutants still exert an inhibiting effecton biogeochemical cycles in the most polluted part of the site.

Acknowledgements

This work was supported by the Région Centre Val de Loire (convention 00087485) and the LabexVol-taire (ANR-10-LABX-100-01).

References

Battaglia-Brunet, F., Dictor, M-C., Garrido, F., Crouzet, C., Morin, D., Dekeyser, K., Clarens, M., and Baranger, P. (2002). An arsenic(III)-oxidizing bacterial population: selection, characterization, and performance in reactors. Journal of Applied Microbiology *93*, 656–667. DOI: 10.1046/j.1365-2672.2002.01726.x

Baur, W.H. (2012). Rigid frameworks of zeolite-like compounds of the pharmacosiderite structure-type. Microporous and Mesoporous Materials *151*, 13–25. DOI: 10.1016/j.micromeso.2011.11.021

Bausinger, T., and Preuβ, J. (2005). Environmental remnants of the first world war: soil contamination of a burning ground for arsenical ammunition. Bulletin of Environmental Contamination and Toxicology *74*, 1045–1053. DOI: 10.1007/s00128-005-0686-z

Bausinger, T., Bonnaire, E., and Preuß, J. (2007). Exposure assessment of a burning ground for chemical ammunition on the Great War battlefields of Verdun. Science of the Total Environment *382*, 259–271. DOI: 10.1016/j.scitotenv.2007.04.029

Bertrand, H., Poly, F., Van, V.T., Lombard, N., Nalin, R., Vogel, T.M., and Simonet, P. (2005). High molecular weight DNA recovery from soils prerequisite for biotechnological metagenomic library construction. Journal of Microbiological Methods *62*, 1–11. DOI:10.1016/j.mimet.2005.01.003

Bradl, H.B. (2004). Adsorption of heavy metal ions on soils and soils constituents. Journal of Colloid and Interface Science *277*, 1–18. DOI: 10.1016/j.jcis.2004.04.005

Cullen, W.R., and Reimer, K.J. (1989). Arsenic speciation in the environment. Chemical Reviews *89*, 713–764. DOI: 10.1021/cr00094a002

Dixit, S., and Hering, J.G. (2003). Comparison of arsenic(v) and arsenic(iii) sorption onto iron oxide minerals: implications for arsenic mobility. Environmental Science and Technology *37*, 4182–4189.
DOI: 10.1021/es030309t

Drahota, P., and Filippi, M. (2009). Secondary arsenic minerals in the environment: A review. Environment International *35*, 1243–1255.
DOI: 10.1016/j.envint.2009.07.004

Fisher, G.L., Prentice, B.A., Silberman, D., Ondov, J.M., Biermann, A.H., Ragaini, R.C., and McFarland, A.R. (1978). Physical and morphological studies of size-classified coal fly ash. Environmental Science and Technology *12*, 447–451.
DOI: 10.1021/es60140a008

Flemming, C. A., and Trevors, J. T. (1989). Copper toxicity and chemistry in the environment: a review. Water, Air, & Soil Pollution *44*, 143-158.
DOI: 10.1007/BF00228784

Haffert, L., Craw, D., and Pope, J. (2010). Climatic and compositional controls on secondary arsenic mineral formation in high-arsenic mine wastes, South Island, New Zealand. New Zealand Journal of Geology and Geophysics *53*, 91–101.
DOI: 10.1080/00288306.2010.498403

Huang, H., Jia, Y., Sun, G.-X., and Zhu, Y.-G. (2012). Arsenic speciation and volatilization from flooded paddy soils amended with different organic matters. Environmental Science and Technology *46*, 2163–2168.
DOI: 10.1021/es203635s

Hube, D. (2013). Potentialités d'un marquage des eaux souterraines par des substances pyrotechniques en relation avec les zones de combats de la première guerre mondiale – Le cas des perchlorates. Rapport final. BRGM/RP-62008-FR. 26p.

Hupy, J.P., and Schaetzl, R.J. (2008). Soil development on the WWI battlefield of Verdun, France. Geoderma *145*, 37–49.
DOI: 10.1016/j.geoderma.2008.01.024

Kim, M.-J. (2001). Separation of inorganic arsenic species in groundwater using ion exchange method. Bulletin of Environmental Contamination and Toxicology *67*, 0046–0051.

DOI: 10.1007/s00128-001-0089-8

Le Forestier, L., and Libourel, G. (1998) Characterization of flue gas residues from municipal solid waste combustors. Environmental Science and Technology*32*, 2250-2256.
DOI: 10.1021/es980100t

Kumar, N., Millot, R., Battaglia-Brunet, F., Négrel, P., Diels, L., Rose, J., and Bastiaens, L. (2013). Sulfur and oxygen isotope tracing in zero valent iron based In situ remediation system for metal contaminants. Chemosphere *90*, 1366–1371.
DOI:10.1016/j.chemosphere.2012.07.060

Lescure, T., Moreau, J., Charles, C., Ben Ali Saanda, T., Thouin, H., Pillas, N., Bauda, P., Lamy, I., and Battaglia-Brunet, F. (2015). Influence of organic matters on As(III) oxidation by the microflora of polluted soils. Environmental Geochemistry and Health. In press.
DOI: 10.1007/s10653-015-9771-3

Magalhâces, M.C.F., Pedrosa De Jesus, J.D., and Williams, P.A. (1988). The chemistry of formation of some secondary arsenate minerals of Cu(II), Zn(II) and Pb(II). Mineralogical Magazine *52*, 679-690.

Masscheleyn, P.H., Delaune, R.D., and Patrick, W.H. (1991). Effect of redox potential and pH on arsenic speciation and solubility in a contaminated soil. Environmental Science and Technology *25*, 1414–1419.
DOI: 10.1021/es00020a008

Morin, G., Lecocq, D., Juillot, F., Calas, G., Ildefonse, P., Belin, S., and Borensztajn, S. (2002). EXAFS evidence of sorbed arsenic (V) and pharmacosiderite in a soil overlying the Echassières geochemical anomaly, Allier, France. Bulletin de la Société Géologique de France *173*, 281-291.
DOI: 10.2113/173.3.281

Murayama, N., Yamamoto, H., and Shibata, J. (2002).Mechanism of zeolite synthesis from coal fly ash by alkali hydrothermal reaction. International Journal of Mineral Processing *64*, 1–17.
DOI: 10.1016/S0301-7516(01)00046-1

Park, J.H., Lamb, D., Paneerselvam, P., Choppala, G., Bolan, N., and Chung, J.-W. (2011). Role of organic amendments on enhanced bioremediation of heavy metal(loid) contaminated soils. Journal of Hazardous Materials *185*, 549–574.
DOI: 10.1016/j.jhazmat.2010.09.082

Pierce, M.L., and Moore, C.B. (1982). Adsorption of arsenite and arsenate on amorphous iron hydroxide. Water Research *16*, 1247–1253.
DOI: 10.1016/0043-1354(82)90143-9

Querol, X., Moreno, N., Umaña, J., Alastuey, A., Hernández, E., López-Soler, A., and Plana, F. (2002). Synthesis of zeolites from coal fly ash: an overview. International Journal of Coal Geology *50*, 413–423.
DOI: 10.1016/S0166-5162(02)00124-6

Rey, A., Petsikos, C., Jarvis, P.G., and Grace, J. (2005). Effect of temperature and moisture on rates of carbon mineralization in a Mediterranean oak forest soil under controlled and field conditions. European Journal of Soil Science *56*, 589–599.
DOI:10.1111/j.1365-2389.2004.00699.x

Saada, A., Breeze, D., Crouzet, C., Cornu, S., and Baranger, P. (2003). Adsorption of arsenic (V) on kaolinite and on kaolinite–humic acid complexes. Chemosphere *51*, 757–763.
DOI:10.1016/S0045-6535(03)00219-4

Santini, J.M., Sly, L.I., Schnagl, R.D., and Macy, J.M. (2000). A new chemolithoautotrophic arsenite-oxidizing bacterium isolated from a gold mine: phylogenetic, physiological, and preliminary biochemical studies. Applied and Environmental Microbiology *66*, 92–97.
DOI:10.1128/AEM.66.1.92-97.2000

Shigemoto, N., Hayashi, H., and Miyaura, K. (1993). Selective formation of Na-X zeolite from coal fly ash by fusion with sodium hydroxide prior to hydrothermal reaction. Journal of Materials Science *28*, 4781–4786.
DOI:10.1007/BF00414272

Sidenko, N., Gieré, R., Bortnikova, S., Cottard, F., and Pal'chik, N. (2001). Mobility of heavy metals in self-burning waste heaps of the zinc smelting plant in Belovo (Kemerovo Region, Russia). Journal of Geochemical Exploration *74*, 109–125.
DOI: 10.1016/S0375-6742(01)00178-9

Smedley, P., and Kinniburgh, D. (2002). A review of the source, behaviour and distribution of arsenic in natural waters. Applied Geochemistry *17*, 517–568.
DOI:10.1016/S0883-2927(02)00018-5

Stolz, J., Basu, P., and Oremland, R. (2002). Microbial transformation of elements: the case of arsenic and selenium. International Microbiology *5*, 201–207.
DOI:10.1007/s10123-002-0091-y

WHO (1993) Guidelines for drinking water quality. World Health Organization. Geneva. P-41

Supplementary Material

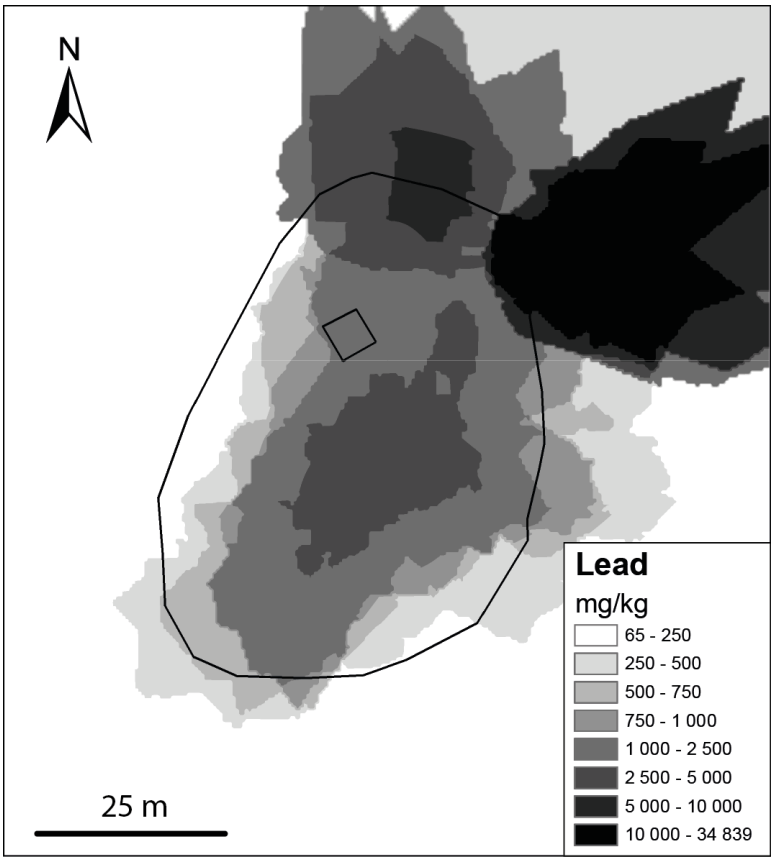

SM1: Map representing the Pb concentration at the soil surface, measured with NITON©.The square represents the hut and the line represents the boundary of the site.

SM2: Particle size fractionsand physical parameters determined for the four soils.

	Particle size fractions			Physical parameters		
Sample	**Coarse sand (%)**	**Fine sand (%)**	**Loam and clay (%)**	**pH**	**Conductivity (mS/cm)**	**Water content**
I	37.0	39.9	23.2	5.34	10.1	0.87
II	18.7	27.5	53.8	5.95	9.2	0.58
III	36.8	26.3	36.9	5.84	10.4	0.31
IV	9.4	36.7	54.0	5.92	10.9	0.91

Coarse sand 2000–200 µm. Fine sand 200–50 µm. Loam and clay <50 µm.

SM3: Phreeqc simulation, integrating the chemistry of solution at the end of the leaching tests. The input data were pH and major and trace concentrations. The calculated saturation indexes are given.

Sample	**I**	**II**	**III**	**IV**
pH	5.34	5.95	5.84	5.92
Water data in mg.L^{-1} (PHREEQC input data)				
As	7.67	4.07	2.18	2.64
Ca	0.83	2.14	2.09	3.62
Cl	1.16	1.82	0.40	0.45
Cu	0.30	0.27	0.27	0.30
F	0.045	0.021	0.041	0.032
Fe	3.89	2.73	3.50	3.08
K	0.26	4.34	1.15	6.36
Mg	0.29	0.27	0.31	0.65
N(-3)	0.0053	0.0003	0	0
N(3)	0	0.149	0	0
N(5)	1.8	3.8	3.99	11.7
Na	0.85	0.78	0.42	0.54
P	0.72	0.22	0.005	0.92
Pb	0.31	0.42	0.44	3.08
S(6)	1.65	1.16	0.66	1.91
Zn	10.3	7.11	6	7.50

Phase	**Saturation index**			
Cupricferrite CuFe2O4	10.69	12.78	3.61	12.81
Cuprousferrite CuFeO2	9.23	10.22	4.15	10.25
Iron(III) hydroxide Fe(OH)3	2.53	3.02	0.02	3.04
Goethite FeOOH	5.23	5.72	2.72	5.74
Hematite Fe2O3	12.85	13.84	7.84	13.88
Magnetite Fe3O4	13.44	14.31	5.43	14.40
Pyromorphite Pb5(PO4)3Cl	8.70	11.49	-21.51	16.86
Strengite FePO4:2H2O	2.54	1.89	-5.62	2.56
Ionic strength	0.0011	0.0012	0.0005	0.0016
Charge imbalance	-44.30	-44.27	-99.62	-44.78

This simulation was performed with PHREEQC Interactive 3.0.6.7757; the data base used was minteq.v4.